13 The role of carbon dioxide and other minor gaseous components and aerosols in the radiation budget

K. Ya Kondratyev and
N. I. Moskalenko
Laboratory of Remote Sensing, Institute for

Abstract

Calculations are presented of the greenhouse effect, which arises from different atmospheric constituents, in particular from CO2, H2O, O3, CH4, NH3, nitrogen oxides and freons. Estimates are made of the mean surface temperature at different epochs during the evolution of the earth's atmosphere. The effect of man's changing activities (especially those resulting in increases in CO2 and freons) are shown to be significant, although our lack of knowledge of different feedbacks including, for instance, the oceans in the climate system means that reliable estimates of these effects cannot yet be made. The presence of aerosol can lead to net heating or cooling, dependent on its type and distribution. In the ozone layer in the stratosphere, complex interactions occur between radiation, photochemistry and dynamics.

13.1 The greenhouse effect

The problem of the impact of radiative factors on atmospheric circulation and climate is central to studies of global energetics of the atmosphere. The radiative regime of the planet is substantially dependent on the chemical composition and turbidity of the atmosphere. As the earth has evolved, the chemical composition and structure of its atmosphere has changed substantially [5, 7, 15, 18]. Climatic changes at present and in the near future can be, to a significant degree, of anthropogenic origin [1-3, 12, 21, 23-35] and therefore the problem of the growing climatic impact of atmospheric pollution is an important aspect of global ecology.

Variations in the concentration and chemical composition of the optically active gaseous and aerosol components of the atmosphere can substantially affect the atmospheric radiation budget and, consequently, the atmospheric circulation. The main mechanism for the climatic impact of radiative factors is ***the greenhouse effect,*** in that the atmosphere, being comparatively transparent to solar radiation, acts as a screen for thermal emission from the planetary surface.

In this chapter, we shall summarise some recent results from studies of the greenhouse effect and its impact on climate; some more-detailed aspects of studies accomplished by 1980 may be found in the references [1-3, 12, 21, 31, 33].

The greenhouse effect may be defined by the difference in temperatures

$$\Delta T = T_s - T_r, \tag{13.1}$$

where T_s, is the temperature of the planetary surface and T_r is a radiative temperature defined by

$$T_r = \left[\frac{F^{\uparrow}}{\sigma}\right], \tag{13.2}$$

where $F^{\uparrow}$ is the outgoing thermal emission flux at the top of the atmosphere and σ is the Stefan Boltzmann constant. In the absence of the atmosphere, $T_r = T_s$ and $\Delta T = 0$.

The globally averaged thermal emission of the planet is characterised by the equilibrium temperature, T_e. In the absence of interior heat sources, the average value of T_r is the equilibrium temperature, T_e, which is determined from the balance averaged over the planet between the absorbed solar energy and outgoing thermal emission, i.e.

$$T_e = [q_0 (1 - A)/4\sigma]^{1/4}, \qquad (13.3)$$

where q_0 is the solar constant for the planet and A is its total albedo.

Calculations of the atmospheric greenhouse effect are presented below. For these calculations the absorption of radiation by atmospheric gases was deduced both from the results of complex measurements of absorption spectra and from direct line-by-line calculations, taking account of the fine structure of the absorption spectra [11]. Optical characteristics of atmospheric aerosols and cloudiness (spectral coefficients of absorption, scattering, and phase function) have been calculated for models of aerosol distributions, both with regard to the chemical composition and the multi-modal size distribution of the aerosol [13, 22].

At present, the radiative regime of the cloudless atmosphere is mainly determined by its water vapour, carbon dioxide, ozone and aerosol, the effect of water vapour in the greenhouse effect being most important.

In between the main absorption bands of CO_2, H_2O and O_3 are 'window' regions where the atmosphere is partially transparent. The most important 'window region' situated near the peak of the black-body curve at terrestrial temperatures is in the region 8–13 μm in wavelength, where continuous absorption due to water vapour occurs and also where absorption bands of minor constituents such as NH, and the freons occur. Although these gases are only present in very small quantities, the absorption bands lead to a noticeable greenhouse effect.

Many processes taking place in the atmosphere are mutually correlated. For instance, an increase in tropospheric temperature is followed by increased water content. The major absorbing components – carbon dioxide and water vapour – exhibit a strong temperature dependence of their spectral transmission functions, and with growing temperature their absorptivity strongly increases. Thus, a rise in the temperature of the troposphere and the surface is followed by intensification of the greenhouse effect mechanism [13].

Calculations show that for a standard model atmosphere, the total greenhouse effect amounts to 33.2 K, with the following contributions from optically active gaseous components: H_2O – 20.6 K; CO_2 – 7.2 K; N_2O – 1.4 K; CH, – 0.8 K; O_3 – 2.4 K; NH, + freons + NO, + CCl_4 + O_2 + N, – 0.8 K.

13.2

Evolution of the greenhouse effect in the earth's atmosphere

It is of interest to follow the evolution of the greenhouse effect and climate on the earth, by modelling the process of radiative heat exchange at different stages of the evolution of the atmosphere's chemical composition.

For these calculations, the data on the vertical ozone profile have been taken from Hart [5], Morss & Kuhn [18], and the vertical profiles for NH, have been drawn from the data on photochemical reactions [12]. The vertical profiles of water vapour concentration have been inferred from that of temperature on the assumption that the atmospheric relative humidity does not exceed 50% at $T_s > 298$ K. Pressure-induced absorption by CO_2, O_2, N_2, NH, were taken from the data of Kondratyev *et al.* [123].

In the early stage of the earth's evolution, its atmosphere contained a large amount of methane and other hydrocarbons reaching 10⁶ atm cm per vertical column. The measurement data of Moskalenko & Parzhin (see [11]) obtained with a multi-path cell with an optical path up to 1 km, have been used in calculations of the spectral transmission functions for such amounts of hydrocarbons. All the absorption bands for methane in the 0.1–25 μm region have been taken into account in calculations.

The mean-global temperature T_s of the planetary surface and the globally averaged greenhouse effect AT are given in Table 13.1 for the models of the chemical composition of the atmosphere given in the same table. According to these models and assuming no variation in the solar constant, the earth's surface was considerably warmer at various stages in its evolution than it is currently, largely due to the increased greenhouse effect arising from substantial

Table 13.1. *Evolution of the greenhouse effect,* AT, *of the earth's atmosphere from the moment of the planet's formation*

Time, 10⁹ years	0	0.2	0.8	1	2	2.5	3.5	4	4.5[a]	5[b]
A	0.15	0.5	0.53	0.53	0.43	0.25	0.29	0.28	0.3	0.33
T_e(K)	235	216	218	219	225	246	253	258	256	253
$C(O_2)$	0	0	.2 4	.2 3	.2 2	.2 i	0.04	0.05	0.2	0.33
$C(N_2)$	0.03	0.1	0.04	0.04	0.40	0.95	0.95	0.95	0.78	0.65
$C(NH_3)$	.3 5	.1 4	.3 4	.25 4	.3 4	.5 6	.25 7	.2 8	.1 9	.3 9
$C(CO_2)$	0.9	0.5	0.1	0.08	0.04	0.02	.5 2	.1 2	.32 3	.32 2
$C(CH_4)$	0.05	0.4	0.83	0.85	0.57	.2 2	.1 5	.18 4	.13 5	.13 5
$W_\perp(O_3)$ (atm cm)	0	0	.3 6	.3 4	.3 3	.3 2	.3 i	0.17	0.3-0.56	0.15
$C(N_2O)$	0	0	0	0	0	.1 7	.1 a	.2 6	.3 6	.6 6
$C(CO)$	0	0	.3 3	.8 3	.4 3	.2 3	.3 4	.8 5	.1 5	.1 4
$W_\perp(H_2O)$ (g/cm²)	2	8.1	22	16	7.1	2	1.4	1.2	1.4	4
P_s (atm)	0.4	1	1.4	1.32	0.73	0.75	0.78	0.8	1	1.18
T_s (K)	296	318	336	328	316	298	288	285	282	306
ΔT (K)	63	102	116	109	91	52	35	27	32	53

.2 4 stands for 0.2 x 10-4 C is the volume concentration; $W_\perp$ is the content of a component in vertical air column; P_s and T_s are the surface pressure and temperature; T_e is the effective temperature of the planet.

(a) Conditions as at present.

(b) A hypothetical model, 5, corrected for possible anthropogenic effect.

quantities of CH,, NH, and **H2O.** The last column of Table 13.1 considers the greenhouse effect due to a hypothetical atmosphere with a substantial increase in CO2 and a decrease of **O3.**

Substantial variations in the greenhouse effect may be expected to occur during periods of volcanic activity arising from changes in gaseous composition and in aerosol content. In studies of evolution of the atmospheric chemical composition during the geological past, considerable temporal variations in carbon dioxide have been discovered connected with volcanic activity [27]. Also, in high volcanic activity conditions it is natural to expect a heightened concentration in the atmosphere of such volatiles as **SO,, H2S** and the presence of a dense haze layer of H2SO4-solution droplets. ***SO,*** is known to have strong absorption bands in the longwave spectral region, coinciding with the atmospheric transparency windows [11] and, consequently, intensifying the greenhouse effect of the atmosphere. At the same time, the presence of the dense sulphate haze at altitudes of 20–30 km with temperatures 200–220 **K** lowers the radiative temperature of the planet and intensifies the greenhouse effect. The ***SO,*** strong absorption bands in the **UV** spectral region could have led to considerable temporal variations in the structural characteristics of the atmosphere in the periods of 'sporadic explosions' of volcanic activity, during which the aerosol of sulphate water solutions had considerably affected the planetary albedo.

13.3

Anthropogenic changes in gaseous constituents and the greenhouse effect

The problem of anthropogenic effects on climate is known to be rather urgent [l-3, 6–10, 12, 16, 17, 21, 23, 27–33]. Most attention has been given to the effect of increased CO2 concentration in the atmosphere, due to the burning of fossil fuel [4,8, 17, 19, 24, 26, 28]. However, growing pollution of the atmosphere causes an increase in concentrations of such components as sulphur dioxide, carbon monoxide, halocarbons, nitrogen oxides, nitric acid, hydrocarbon compounds, etc. Also of great importance is aerosol – both injected directly to the atmosphere and resulting from chemical transformations of gaseous components to solid ones – the effect of aerosol will be considered in the next section. All these components have absorption bands in the IR spectral region and all make some contribution to the greenhouse effect of the atmosphere [3, ***6,*** 12, 16, 21, 29, 31, 33, 34].

First, considering changes of CO2, calculations (the results of which are shown in Table 13.2)have been carried out with a 1-D model of the atmosphere (assuming radiative-convective equilibrium) of the change of surface temperature, ***AT,*** which would occur for increasing CO2 concentration. Two different models have been used, one with fixed water vapour and one allowing the water vapour content **W** g cm-2 of the troposphere to change with surface temperature, *Ts,* according to the expression :

$$W = 1.4 \exp 0.07\,(Ts - 288). \qquad (13.4)$$

Within the troposphere the relative humidity was assumed to be independent of height.

In Table 13.2, it is of interest to note the absence of greenhouse 'saturation' effect, even in the case of a ten-fold CO2 increase.

Fig. 13.1 shows two vertical temperature profiles calculated for the mean global atmosphere of the earth (curve 1) and an atmosphere with the ten-fold increase of the CO2 content (curve 2) as compared to that of the present day. Curve 2 refers to the combined greenhouse effect caused by increased concentrations of CO2 and water vapour. Of interest in Fig. 13.1 are the stratospheric temperature decrease and the growing altitude of the tropopause due to the CO2 greenhouse effect.

The calculations of Table 13.2 have not taken into account the feedback effect of clouds or the effect of atmospheric or oceanic circulation which will be referred to in Section 13.8.

Calculations have also been carried out on the greenhouse effect due to other gaseous constituents. Doubled concentration **of** nitrous oxide N2O leads to a 0.7 **K** rise in the mean temperature, and when concentrations of ammonia and methane are doubled, the surface temperature rises, respectively, by 0.1 and 0.3 **K.** A 20-fold increase of freons can lead to the greenhouse effect reaching

Fig. 13.1. Calculated vertical temperature profiles: (1) for a mean global model of an atmospheric vertical structure and a mean chemical composition; (2) for an atmosphere with a ten-fold increase **of *CO2*** concentration.

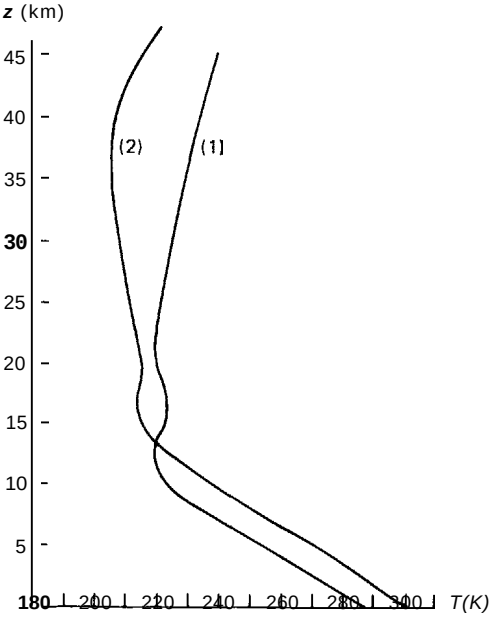

Table 13.2. ***Surface temperature increase AT v. n-fold increase of CO2 Concentration***

n	1	1.5	2	3	4	5	6	7	8	10
AT'	0	1.6	2.4	4.1	5.1	5.7	6.3	6.7	7.2	8.1
AT"	0	2.9	4.4	7.6	9.4	10.4	11.2	11.9	12.6	13.1

AT' and ***AT"*** are values of ***AT*** obtained, respectively, with fixed water-vapour and with varying water-vapour content.

0.6–1 K and the total greenhouse effect due to doubled concentrations of N_2O, CH_4, SO, and HNO, reaches 1.2 K.

The greenhouse effect is also significant in the stratosphere. A doubling of the water-vapour content there leads to a warming by 1 K, and a decrease of O_3 concentration by 25% would lead to a reduction of temperature by 0.4–0.5 K.

The above estimates of the effect of variations in concentrations of minor gaseous components on the temperature, T_s, agree well with the results of other authors [16, 29] and confirm the conclusion that anthropogenic changes in the concentration of a number of minor components, the effect of which on climate had previously been considered negligible, would lead to a possible climate warming in the future. It is therefore important to monitor global trends of the concentration of these minor components.

On the basis of a 1-D global radiative–convective model, similar to our own, Lacis *et al.* [34] have made calculations of surface warming due to the greenhouse effect of anthropogenic changes in the components CO2, chlorofluorocarbons, methane, and nitrous oxide for two cases:

(1) observed rates of injections for the decade 1970–80;

(2) doubled concentrations.

Their results are given in Table 13.3 which shows that the total contribution of methane, chlorofluorocarbons and nitrous oxide is equal to 50–100% of the CO2 contribution. The equilibrium warming for arbitrary changes may be fitted to an analytical expression:

$$T_e\,(\mathrm{K}) = 0.57\,(\mathrm{CH_4})^{0.5} + 2.8\,(\mathrm{N_2O})^{0.6} - 0.057 \times \mathrm{CH_4} \times \mathrm{N_2O} + 0.15 \times \mathrm{CCl_4} + 0.18 \times \mathrm{CCl_2F_2} + 2.5 \ln\left[1 + 0.005\,(\Delta \mathrm{CO_2}) + 10^{-5}\,(\Delta \mathrm{CO_2})^2\right], \quad (13.5)$$

where the abundances are in pprn except for CCl_3F and CCl_2F_2, which are in ppb, and the CO, amount is in ppm above a reference value of 300 ppm. This equation fits the model results to better than 5% for abundances CH, < 5 ppm, N_2O < 1 ppm, CCl_2F < 2 ppb, $CClF_3$ < 2 ppb and A CO, < 300 ppm; the third term corrects for overlap of CH, and N_2O bands.

Lacis *et al.* [34] point out that their estimates do not take into account the atmosphere-ocean interaction, which slows down the climate warming due to the greenhouse effect [see 4, 17]. In the case of the interaction of the atmosphere with the upper mixed oceanic layer of about 100 m depth, the surface temperature rise by 1970 would be half i.e. ≈ 0.1 °C, or ≈ 0.14.2 °C if atmospheric pollution before 1970 is taken into account. Since such a level of temperature increase is close to the natural mean-global temperature fluctuations on decadal timescales, the anthropogenic impact on climate cannot yet be observed with any certainty. But because total warming for the 1970s, 1980s and 1990s may reach 0.2–0.3 °C it may become observable by the year 2000.

Considering possible climatic changes due to anthropogenic variations in the chemical composition of the atmosphere, one should bear in mind the interrelationship of various climatological factors. For instance, an increase in the chlorofluorocarbon content can substantially change the atmospheric ozone concentration. Therefore, atmospheric temperature variations have been calculated [12] taking account of the vertical profile of ozone resulting from photochemical reactions between ozone and chlorofluoromethanes.

It is important to take into account ozone variations not only in the stratosphere, but also in the troposphere, since variations in tropospheric ozone often lead to opposite effects as compared to those arising from stratospheric disturbances of ozone concentration. Observations exist indicating that upper tropospheric ozone concentration has increased 20–25% during the past 15 years (Attmanspacher 1982, unpublished result) so that special attention should be given to the tropospheric ozone problem.

13.4 The effect of aerosol

In considering the effect of aerosol on the radiative regime of the atmosphere, the mechanisms for radiation scattering and absorption by aerosol have to be taken into account [3, 13]. Depending on the aerosol optical density, its size distribution and chemical composition, and also depending on the surface albedo, conditions may appear when radiation processes due to aerosol can either raise or lower the albedo of the earth–atmosphere system. The presence of aerosol can lead to an increase of surface temperature due to a positive greenhouse effect or to a lowering of the surface temperature (referred to as an anti-greenhouse effect).

Figure 13.2 shows the vertical profile of atmospheric aerosol optical density for a mean-global atmosphere assumed in the calculations. A fine disperse background aerosol consists of 80% particles of gas-to-particle conversion origin and 20% small-sized dust particles. The tropospheric aerosol contains 40% mineral dust, 20% water solution of sulphates, 20% industrial aerosols, and 20% sea salt. The stratospheric aerosol layer is represented by the 75% H_2SO_4 water solution particles. Optical characteristics of

Table 13.3. *Greenhouse effects of several trace gases*

Species	Arbitrary change			1970–80 change		
	a_0(ppb)	Δa(ppb)	ΔT_e (°C)	a_0(ppb)	Δa(ppb)	ΔT_e (°C)
CH_4	1600	1600	**0.26**	1500	**150**	0.032
	280	280	**0.65**	295	**6**	0.016
CCl_3F	0	2	0.35	**0.045**	0.135	0.020
CCl_2F_2	0	2	**0.36**	0.125	0.190	0.034
CO,	300000	300000	2.9	**325000**	12000	0.14

a, (Aa): initial (increase of) concentration.
AT: temperature rise.

aerosol formations have been considered by Moskalenko *et al.* [22]; examples are given in Table 13.4 of ω_0, the single scattering albedo in the wavelength region 0.3–1.7 μm for industrial, background and mineral aerosols.

For small-sized background aerosol particles in the IR spectral region, the absorption coefficient σ_a exceeds the scattering coefficient σ_s; for wavelengths $\lambda > 1$ μm the extinction coefficient is mainly determined by aerosol absorption. Therefore, small-sized aerosol warms up the atmosphere due to solar radiation absorption and also emits in the longwave spectral region, thereby screening thermal emission from the surface. The small-sized background aerosol, like an absorbing gaseous component, intensifies the greenhouse effect of the atmosphere, raising the surface temperature by 3 K for mean-global conditions.

The above estimates of the greenhouse effect for the small-sized fraction of the atmospheric aerosol are partially compensated for by the anti-greenhouse effect of the coarse fraction of the tropospheric aerosol which amounts to $\Delta T = -1.4$ K for the model of Fig. 13.2. The anti-greenhouse effect ($\Delta T_s = -0.5$ K) is also typical of the stratospheric sulphate aerosol layer. However, for the planet on the average, the greenhouse effect due to the strongly absorbing small-sized aerosol fraction probably dominates the anti-greenhouse effect of coarse aerosol particles.

Atmospheric pollution due to man's activity raises the concentration of strongly absorbing aerosol particles (Table 13.3), which does not lead to substantial variations in the planetary albedo but increases the screening of the outgoing thermal emission of the surface. An increase by a factor of 1.5 of the tropospheric aerosol concentration due to man's activity will warm the surface by 1.7 **K** through the greenhouse effect. A doubled optical thickness of the stratospheric background aerosol (through an increasing number of free carbon-containing particles) will raise the temperature, &, by 0.8 **K.**

Fig. 13.2. The vertical structure of the optical density for (1) the atmospheric aerosol; and (2) background aerosol; (3, **4**) the models of the optical density of cirrus clouds, assumed to cover $\frac{1}{10}$ and & of the sky with the upper level clouds.

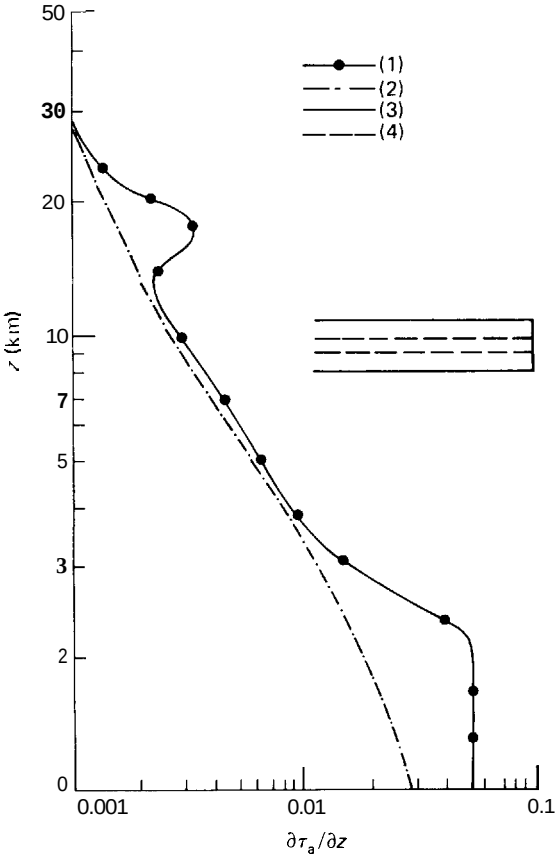

Table 13.4. ***Single scattering albedo ω_0 for different types of aerosols***

Wavelength *(μm)*	0.3	0.5	0.69	1.06	1.7
Industrial aerosol	0.621	0.603	0.592	0.660	*0.640*
Mineral aerosol	0.776	0.864	0.892	0.952	0.956
Background aerosol	0.660	0.720	0.560	0.260	0.090

13.5

The effect of cloud cover

Clouds are the most important factor governing the radiative regime of the earth. Growing cloudiness raises the albedo and reduces the solar radiation flux reaching the earth's surface. On the other hand, the presence of cloudiness lowers the radiative temperature corresponding to the outgoing radiation, leading to a positive greenhouse effect. At night, this positive greenhouse effect is important but during the daytime, over surfaces that are not snow covered, it is likely that the cooling due to increased albedo dominates over the greenhouse effect. However, in winter conditions (the earth's surface is covered with snow) the presence of clouds does not substantially change the albedo, and the greenhouse effect in these conditions is dominant.

Due to anthropogenic causes, the structural and optical characteristics of the earth's cloud cover can be changed substantially. In particular, flights of supersonic aircraft can lead to an increase in the upper-level cloud cover and hence to radiative cooling. At present it is difficult to foresee the scale of the greenhouse effect due to this factor.

Some calculations have been carried out of variations in the surface temperature, Ts caused by increasing upper-level cloud amount (upper troposphere, lower stratosphere). The results depend strongly on selected models of the cloud cover (Fig. 13.2), and lie within the range -0.7 to 3 K. The value -0.7 **K** corresponds to clouds of 1 km thickness with their base at 9 km and the value -3K corresponds to clouds of 3 km thickness with their base at 8 km.

13.6

The earth–atmosphere system albedo

The earth–atmosphere system albedo is known to depend substantially on latitude and is determined by surface reflectivity, cloud amount, and absorbing and scattering properties of the atmospheric gas phase. Different types of the surface have drastically different albedos. For instance, the sea surface albedo, A, is about 0.1, the vegetation cover albedo is close to 0.4, and the snow albedo can reach 0.84.9. Albedos of different types of clouds vary strongly depending on the location of the sun in the sky. Table 13.5 lists the dependences of the albedo, A, on the solar zenith angle

calculated using the Eddington approximation for different values of the surface albedo and optical thickness of mineral aerosols. In these tables, reflectivity $A = 0.1$ corresponds to the sea surface, $A = 0.4$ to the vegetation cover, and $A = 0.7$ to dense clouds or snow-covered surface.

For the sea surface, the aerosol raises the albedo, A, of the surface–atmosphere system but in the case of the snow-covered surface or the overcast sky, the albedo decreases considerably. If the underlying surface is the vegetation cover, then with increasing atmospheric turbidity the albedo becomes lower at solar zenith angles $0 < 60''$ and becomes larger when solar zenith angles are high. Table 13.6 illustrates the effect of industrial aerosol on the system albedo. For most solar zenith angles, the growing atmospheric turbidity due to industrial aerosol, causes a decrease of the surface–atmosphere system albedo.

For a cloudless atmosphere in the absence of dust clouds, the albedo over water bodies grows if the imaginary part of the complex index of refraction $x < 0.015$. The situation, however, changes drastically in the presence of clouds over water bodies. First, the marine aerosol, as a rule, is located below the upper boundary of the cloud cover, and its optical effect is screened by cloudiness. Second, the albedo of the sea surface–cloud system increases drastically. Because of the latter, the presence of aerosol in the troposphere above the cloud cover lowers the albedo. The albedo decreases still lower if the aerosol absorbs shortwave radiation. The latter occurs in a real atmosphere, since the above-cloud aerosol is an ensemble of dry particles of the mean-global salt and mineral dust.

The above-cloud dust aerosol with an optical thickness $\tau = 0.2$ lowers the albedo of the earth–atmosphere system by 3%. Over the oceans, the effect of the atmospheric aerosol on the albedo is determined by the cloud amount. In the atmosphere, with overcast cloudiness, the presence of aerosol always decreases the albedo, regardless of the surface type. A similar conclusion holds for a cloudless atmosphere and snow-covered surface.

For the continents, when the land is covered with vegetation, and there are no clouds, the effect of aerosol on the total albedo is practically absent in the range of optical thicknesses of the atmospheric aerosol 0.05–0.5. The latter means that only the vertical distribution of the shortwave radiation balance changes. With growing atmospheric turbidity, absorption of shortwave radiation by the surface decreases, and by the atmosphere increases.

For industrial regions with surface reflectivity of **0.3,** the industrial aerosol, characterised by the albedo of single scattering $\tau_s/\sigma_a = 0.6$ and optical thickness $\tau = 0.4$, lowers the albedo, A, by 20% in the absence of clouds.

It is of interest to estimate the effect of dust transport from deserts on the radiative regime. Calculations have shown that a dust cloud decreases the planetary albedo, on the average, due to

Table 13.5. ***The dependence of the surface–atmosphere system albedo, A, on its determining factors at the 0.55 μm wavelength for dust aerosol.***

Θ°	$A_s = 0.1$ $\tau = 0.2$	$A_s = 0.1$ $\tau = 0.5$	$A_s = 0.1$ $\tau = 1.0$	$A_s = 0.7$ $\tau = 0.2$	$A_s = 0.7$ $\tau = 0.5$	$A_s = 0.7$ $\tau = 1.0$	$A_s = 0.4$ $\tau = 0.2$	$A_s = 0.4$ $\tau = 0.5$	$A_s = 0.4$ $\tau = 1.0$
	$A(\Theta)$								
0	**0.12**	**0.14**	**0.18**	**0.65**	**0.60**	**0.51**	**0.37**	**0.35**	**0.33**
30	**0.15**	**0.17**	**0.23**	**0.66**	**0.59**	**0.52**	**0.39**	**0.37**	**0.36**
60	**0.18**	**0.22**	**0.30**	**0.68**	**0.60**	**0.53**	**0.41**	**0.40**	0.40
70	**0.22**	**0.29**	**0.36**	**0.69**	**0.62**	0.55	**0.44**	**0.44**	**0.46**
80	**0.30**	**0.42**	**0.48**	**0.70**	**0.64**	**0.60**	**0.50**	**0.52**	**0.52**
85	**0.41**	**0.50**	**0.51**	**0.72**	**0.67**	**0.63**	**0.55**	**0.60**	**0.56**
90	**0.52**	**0.56**	**0.58**	**0.74**	**0.72**	**0.66**	**0.64**	**0.64**	**0.62**

Here $\sigma_a^s/\sigma_a = 0.9$; A, is the surface albedo; τ is the optical thickness; Θ is the solar zenith angle.

Table **13.6.** ***The dependence of the surface–atmosphere system albedo, A, on its determining factors at the 0.55 μm wavelength for industrial aerosol.***

Θ°	$A_s = 0.1$ $\tau = 0.2$	$A_s = 0.1$ $\tau = 0.5$	$A_s = 0.1$ $\tau = 1.0$	$A_s = 0.7$ $\tau = 0.2$	$A_s = 0.7$ $\tau = 0.5$	$A_s = 0.7$ $\tau = 1.0$	$A_s = 0.4$ $\tau = 0.2$	$A_s = 0.4$ $\tau = 0.5$	$A_s = 0.4$ $\tau = 1.0$
	$A(\Theta)$								
0	**0.09**	**0.08**	**0.07**	**0.57**	0.44	**0.28**	**0.33**	**0.26**	**0.20**
30	**0.10**	**0.09**	0.09	**0.57**	**0.41**	**0.27**	**0.34**	**0.26**	**0.21**
60	**0.11**	**0.10**	**0.10**	**0.55**	**0.38**	**0.26**	**0.35**	**0.27**	**0.23**
70	**0.13**	**0.13**	**0.14**	**0.54**	**0.37**	**0.27**	**0.36**	**0.28**	**0.25**
80	**0.18**	**0.20**	**0.20**	**0.53**	**0.36**	0.28	**0.38**	**0.32**	**0.29**
85	**0.23**	0.26	**0.24**	**0.51**	**0.42**	**0.35**	**0.41**	0.40	**0.36**
90	**0.30**	**0.32**	**0.28**	**0.49**	**0.47**	**0.45**	**0.44**	***0.46***	**0.40**

Here $\sigma_a^s/\sigma_a = 0.7$; A, is the surface albedo; τ is the optical thickness; Θ is the solar zenith angle.

shortwave radiation absorption. If a dust cloud with an optical thickness $\tau_a = 0.4$ covered the whole planet, its albedo would have decreased by 16%. Since the dust cloud can cover about 0.1 of the planetary area, the planetary albedo can decrease by 1.6%. The latter is equivalent to a rise of the radiative temperature of the planet by about 0.8 K. Calculation of surface temperature change in the approximation of radiative-convective equilibrium, using a scheme suggested by Kondratyev & Moskalenko [15] gives an increase of the mean global temperature for this case of 2.1 K. Thus the growing dust load of the troposphere is an important climate-forming factor not only on the regional scale, but also on the planetary scale.

13.7

Feedback factors

The studies which have been mentioned so far have employed simple 1-D models and have not taken into account dynamical processes, the influence of the oceans, or feedback processes such as those which occur through cloud–radiation interaction. Predictions with a 3-D general circulation model of the atmosphere of the effect of a doubling of the CO, content of the atmosphere have been carried out by Manabe & Wetherald [8] who find an increase in surface temperature of about 2 K in the tropics, 3 K in mid-latitudes and up to 8 K in polar regions.

Mitchell *et al.* [35] have undertaken numerical climate modelling for cases of normal (320 ppm) and doubled CO, concentration on the basis of the Lawrence Livermore National Laboratory Statistical Dynamical Model. They have made estimates of the sensitivity of the earth radiation budget and its components, namely absorbed solar radiation ***(S)***, outgoing longwave radiation *(F)* and net total flux ***(R)*** to changes in surface temperature ***(T)***, precipitable water vapour *(r)* total cloud cover fraction ***(C)***, surface albedo ***(A)***, and CO, concentration. Table 13.7 shows the changes to be expected in the various parameters when the CO, increases; Table 13.8 shows the changes in ***S***, F and ***R*** which would occur due to the change in each parameter. Warmer temperatures lead to an increase of ***F*** hut do not change ***S***, while the increase in water vapour absorbs more of the solar and longwave radiation, increasing ***S*** but reducing ***F***.

Of great interest is the strong hemispheric difference in the effect of precipitable water on solar radiation in spite of the symmetry for longwave radiation. This situation is determined by the fact that solar radiation is absorbed primarily by water vapour in the lower troposphere, its content being larger in the northern hemisphere (NH) than in the southern hemisphere **(SH).** Since CO, doubling creates some decrease of cloud amount in the NH and some increase in the **SH,** consequent changes of absorbed solar radiation take place.

An important fact in the longwave radiation changes is the spatial (latitudinal and altitudinal) redistribution of cloudiness. Surface albedo variations are due only to soil moisture changes. The impact of ice albedo feedback does not show itself, because sea ice extent has not been allowed to change in the model.

Mitchell *et al.* proceed in their paper to discuss the effect of multiple feedbacks i.e. changes in more than one parameter at a time. It is clear from their study that further study of the various feedback processes is required before more-definite estimates can be made of the effect of changes in atmospheric CO,. In particular, much-better understanding is required of the feed back effect of clouds on the various radiation components and of the influence of the ocean circulation on the various changes. For the latter studies, coupled atmospheric ocean models will be required.

13.8

Interactions in the stratosphere between radiation, photochemistry and dynamics

The problem of the interaction between radiation, photochemistry and dynamics is relevant to climate studies, especially in the stratosphere. In the pioneering paper by Bojkov [9], the interaction between the patterns of ozone distribution and of the stratospheric circulation have been studied. Since that time, a large number of investigations have been carried out on various feedback relationships. To describe these in detail is outside the scope of this chapter; many of them have been reviewed in monographs and

Table 13.7. *Hemispheric and globally averaged changes in various parameters (doubled-CO, run minus control run)*

Parameter	Control case	Change
Surface temperature T (K)		
NH	285.2	2.333
SH	289.1	0.514
G	287.2	1.424
Precipitable water vapor r (gcm-2)		
NH	2.1	0.251
SH	2.3	0.190
G	2.2	0.220
Total cloud cover fraction C		
NH	0.56	−0.005
SH	0.54	0.027
G	0.55	0.011
Surface albedo A		
NH	0.23	−0.007
SH	0.13	−0.002
G	0.18	−0.004
CO, concentration (ppmv)		
NH	320.0	320.0
SH	320.0	320.0
G	320.0	320.0

Table 13.8. *Hemispheric and globally averaged changes (doubled CO, minus control) in net downward solarflux* (δS), *net upward longwaveflux* (δF) *and in net total flux* (δR) *at the top of the atmosphere due to each of the fivefactors listed in the column headings. All values in Wm-2*

	T	*r*	*C*	*A*	CO2
δS					
NH	0.000	0.569	1.906	0.501	0.000
SH	0.000	0.120	−3.048	0.285	0.000
G	0.000	0.344	−0.571	0.393	0.000
δF					
NH	4.359	−1.823	1.570	0.000	−2.454
SH	2.700	−1.657	−0.041	0.000	−2.640
G	3.530	−1.740	0.764	0.000	−2.547
δR					
NH	−4.359	2.392	0.335	0.501	2.454
SH	−2.700	1.777	−3.007	0.285	2.640
G	−3.530	2.085	−1.336	0.393	2.547

papers [3, 12, 14, 21]. However, a brief description will be given of recent work by Haigh & Pyle [20].

Using a 2-D general circulation model at Oxford University, Haigh & Pyle modelled, numerically, various possible anthropogenic impacts on the ozone layer and the associated climate changes. Their model provides for chemical, radiative and dynamical interactive processes in the stratosphere and reproduces, for example, the feedback effects between temperature (through temperature dependence of the chemical reaction rates), changes in circulation and variations in the ozone concentration. Since the upper stratospheric ozone content is negatively correlated with temperature, stratospheric cooling arising from CO, increase will be greater than in the absence of ozone.

The model extends from the surface to approximately 80 km. Zonal mean temperatures, wind vector components and concentrations of gas constituents are held as functions of time, latitude and altitude (log pressure) with resolutions of four hours, 9.47° of latitude and 0.5 in. log pressure (about 3.5 km). At each time step, the meridional circulation necessary to preserve the geostrophic balance against the perturbing effects of heating and eddy transports of momentum and heat is calculated.

The photochemical scheme in the model includes 50 reactions describing the oxygen, hydrogen, nitrogen, and chlorine cycles (the natural chlorine cycle is excluded). Component concentrations for the following families are calculated: (O^1D), O_x and O_3; N, NO, NO, and $ClONO_2$; HNO_x; H_2O_2; H, OH and HO_x; Cl, ClO, $ClONO_x$, and HCl; $CFCl_3$; CF_2Cl_2 (within each group photochemical equilibrium is assumed). Invariant profiles of H_2O, CH_4, H_2, N_2O and CO are specified independent of latitude. Although some of the rate constants have since been updated, the values assumed in the model were adequate for examining the coupling between the radiation, photochemistry and dynamics.

Particular attention was paid to providing an adequate radiation parameterisation scheme. Between the tropopause and 25 km, radiative equilibrium was assumed because of the impossibility of making sufficiently accurate calculations of the heating rates in this region where large terms of opposite sign nearly cancel. Fixed heating rates are used in the troposphere.

Four model runs were made:

(A) control (chlorine cycle excluded, CO, mixing ratio of 320 ppmv assumed);

(B) CO, volume mixing ratio increased up to 625 ppmv;

(C) chlorofluorocarbon (CFC) injections taken at four times the average 1973–76 production rate;

(D) simultaneous doubling of CO, content and CFC injection.

Comparing the control run with observational data demonstrated a sufficient agreement to give plausibility to the model, although there are significant differences (e.g. too low winter polar temperatures, overestimated zonal winds, high total ozone at the equatorial minimum).

The (B) run was performed in three steps with CO, mixing ratios, respectively, of 400, 500 and 625 ppmv considered appropriate for the years 2000, 2020 and 2040 AD. Doubling of CO, brings about considerable (up to 10–12 K) decrease in the upper stratospheric temperatures, coupled with a 20–25% increase in O_x concentration. The effect on zonal circulation is also pronounced; however, the meridional transport remains practically unperturbed.

The total O_3 suffers strong increase (about 20%) near the north pole in summer, and a weaker one of 14% in southern hemisphere high latitudes, this difference reflecting the asymmetry in the global ozone field. The global increase in total O_x is around 9%, considerably larger than any of the values predicted by the 1-D models which fail to account for the dynamics of the lower stratosphere. The major source region of NO_x is at around 30 km.

Injections of CFCs (run C) reduce the temperatures by up to 8–10 K and, contrary to the effect of doubling the CO, simultaneously deplete O_3 concentration by as much as 35% around 40 km, with a corresponding decrease in the total O_3. The joint perturbation (CO_2 + CFCs) results presented in Table 13.9 show that their separate effects on the total O_3 are not additive. For example, addition of those effects would lead to the total O_x depletion by only 4% around 2040, while the more accurate calculation for the joint effect produces the figure of 8.1%. Qualitatively, the results are similiar for ozone concentrations at different levels (i.e. interactive drop is considerably less than additive).

The interactive temperature decrease, peaking in excess of 20 K in the upper stratosphere, leads to substantial changes in the zonal circulation. Non-linearity of the interactive effect is due to the varying temperature dependences of the ozone concentration for the different models, namely: $d \ln(O_3)/d(T^{-1}) =$ 1188 K(A); 1172 K(B); 557 K(C); 461 K(D). The data in Table 13.10 characterise the relative importance of each chemical cycle in depleting the total ozone at the equator near 40 km in April 2045. These data testify to the importance of the chlorine cycle.

13.9

Conclusions

This paper has considered the present status of our knowledge regarding the impact of atmospheric composition changes on the earth's radiation budget and on climate. Further research is

CO, content (ppmv)	zero CFC	CFC increases predicted for year (2000)	(2020)	(2040)
320	0	−3.2	−8.3	−12.8
400	+3.0	−0.6		
500	+5.9		−4.1	
625	+8.8			−8.1

Cycle	Run (A)	(B)	(C)	(D)
pure oxygen	26.3	24.4	6.6	4.5
HO_x	17.9	19.6	9.5	8.7
NO_x	55.8	56.0	30.0	25.9
ClO_x	0	0	53.9	60.9

required in two key areas:

(1) the prediction of changes of composition including the spatial–temporal variations of different components through increased knowledge and understanding of biogeochemical cycles (see Chapter 12);

(2) adequate modelling of detailed atmospheric processes including the interactions between radiation, chemistry and dynamics.

The pursuit of research in these areas is an important component of the World Climate Research Programme.

References

[1] Borisenkov, E. P. 'Climate studies and their application aspects'. ***Meteorol. and Hydrol., 1981, 6,*** 32-48 (in Russian).

[2] Budyko, **M. I.** ***Climate in the Past and Future.*** Leningrad, Gidrometeoizdat, 1980, 351 pp. (in Russian).

[3] Kondratyev, K. Ya. ***Radiative Factors of the Present-Day Global Climate Change.*** Leningrad, Gidrometeoizdat, 1980, 279 pp. (in Russian).

[4] Cess. R. D. & Goldenberg, **S.** D. 'The effect of ocean heat capacity upon global warming due to increasing atmospheric carbon dioxide'. **J.** ***Geophys. Res.,*** 1981. **C86** (l), 498–502.

[5] Hart. M. A. 'The evolution of the atmosphere of the Earth'. ***Zcarus,*** 1978. **33** (l), 23–39.

[6] Houghton, J. T. 'Greenhouse effects of some atmospheric constituents'. ***Phys. Trans. Roy. Soc., London,*** 1979, **A290,** (1376), 515–21.

[7] Kondratyev, K. Ya. & Hunt G. E. ***Weather and Climate on Planets.*** Pergamon Press, Oxford, 1982, 755 pp.

[8] Manabe. **S.** & Wetherald, R. T. 'On the distribution of climate change resulting from an increase in CO2 content of the atmosphere.J. ***Atmosph. Sci.,*** 1980, *37* (l), 99–118.

[9] Bojkov, R. D. 'Planetary study of the ozone heating of the stratosphere'. ***Bull. of the Cairo Meteorol. Department,*** 1979, 1, 193-244.

[l0] Fels. **S.** B., Mahlman, **J.** D., Schwarzkopf, M. D. & Sinclair, R. W. .Stratospheric sensitivity to perturbations of ozone and carbon dioxide: radiative and dynamical response'. J. ***Atmosph. Sci.,*** 1980, **37** (l0), 2265-97.

[12] Kondratyev, K. Ya. ***Stratosphere and Climate. Progress in Sci. and Technol., Meteorol. and Climatol.,*** Moscow, VINITI, 1981, Vol. 6. 223 pp. (in Russian).

[13] Kondratyev, **K.** Ya., Moskalenko, N. I., Terzy V. F. & Skvortfsova, **S.** Ya. 'Modeling of the optical characteristics of the atmospheric aerosols'. ***In : Polar Aerosol, Extended Cloudiness, and Radiation.*** FGGE Ser., Vol. 2, Leningrad, Gidrometeoizdat, 1981, pp. 130-53. (in Russian).

[14] Hartmann, D. L. 'Some aspects of the coupling, between radiation, chemistry and dynamics in the stratosphere'. ***J. Geophys. Res.,*** 1981, **C86** (l0), 9631-40.

[1 5] Kondratyev, K. Ya., Moskalenko, N. I. 'The greenhouse effect of planetary atmospheres'. ***Nuovo Cimento*** C, 1980, **30** (4), 436-60.

[16] Ramanathan, V. 'Climate effects of anthropogenic trace gases'. ***In: Interactions of Energy and Climate,*** eds. B. Bach, **J.** Pankrath & **J.** Williams, Reidel, Dordrecht, Netherlands, 1981, pp. 269–80.

[17] Gates, W. L., Cook K. H. & Schlesinger, M. E. 'Preliminary analysis of experiments on the climatic effects of increased CO2 with the atmospheric general circulation model and a climatological ocean'. ***J. Geophys. Res.,*** 1981, ***C86*** (7), 6385-93.

[18] Morss, D. A. & Kuhn, W. R. 'Paleoatmospheric temperature structure'. ***Zcarus,*** 1978, ***33*** (1), 4 0 - 9 .

[19] Vupputuri, R. K.-R. The Effect of Increased Atmospheric CO2 on Stratospheric Temperature Structure and Ozone Distribution Investigated in a 2-D Timedependent Model. ***Canadian Climate Center, Report No. 7,*** 1981.

[20] Haigh, J. D. & Pyle, J. A. 'Ozone perturbation experiments in a two-dimensional circulation model'. ***Q.*** J. ***Roy. Meteorol. Soc.,*** 1982, 108 (457), 551–74.

[21] Kondratyev, **K.** Ya. The Present State, Perspectives, and the Role of Observations from Space. ***Progress in Sci. and Technol., Meteorol. and Climatol.*** Moscow, VINITI, 1982, Vol. **8,** 274 **pp.**

[22] Moskalenko, N. I., Tantashev, M. V., Terzy, V. F. & Skvortsova, **S.** Ya. 'The optical characteristics of the atmospheric aerosols'. ***In: Aerosols and Climate.*** FGGE Ser., Vol. 1, Leningrad, Gidrometeoizdat, 1981, pp. 154-65 (in Russian).

[23] Ramanathan, V. 'Climatic effects of ozone change: a review'. ***Low Latitude Aeron. Processes. Proc. Symp. 22nd Planetary Meet., COSPAR.,*** Bangalore, 1979, Oxford, 1980, pp. 223–36.

[24] Reck, R. A. 'Carbon dioxide and climate: comparison of one- and three-dimensional models'. ***Environ. Int.,*** 1980, ***2 (4-6),*** 387–91.

[25] Schneider, **S.** H. & Thomson, **S.** L. 'Cosmic conclusions from climatic models: can they be justified?' ***Icarus,*** 1980, 41 (3), 456-69.

[26] Hummel, J. R., Reck, R. A. 'Carbon dioxide and climate: the effects of water transport in radiative-convective models'. J. ***Geophys. Res.,*** 1981, **C86** (12), 12035-38.

[27] 'The problems of atmospheric carbon dioxide'. ***Proc. of the Soviet-American Symp., Dushanbe,*** 12–20, October 1978, Leningrad, Gidrometeoizdat, 1980, 286 pp. (in Russian).

[28] Pittock, **A.** B. & Salinger, **M. J.** 'Towards regional scenarios for a CO2- Earth'. ***Clim. Change,*** 1982, 4 (l), 23–40.

[29] Wang, W. **S.,** Yung, T. L., Lacis, A. A., Mo, T. & Hansen, T. E. 'Greenhouse effects due to man-made perturbations of trace gases'. ***Science,*** 1976, 194 (4266), 685-91.

[30] Kukla, G. & Gavin, J. 'Summer ice and carbon dioxide'. ***Science,*** 1981, 214, 497–503.

[31] Alexandrov, E. L., Karol, I. **L.,** Rakipova, L. R., Sedunov Ya. **S.** & Khrgian A. Kh. ***Atmospheric Ozone and Changes of Global Climate.*** Leningrad, Gidrometeoizdat, 1982, 167 pp. (in Russian).

[32] Hadden, R. A. & Ramanathan, V. 'Detecting climate change due to increasing carbon dioxide'. ***Science,*** 1980, ***209*** (4458), 763–7.

[33] Kellogg, W. W. & Schware, R. ***Climate Change and Society: Consequences of Increasing Atmospheric Carbon Dioxide.*** Westview Press, Inc., Boulder, Colo., 1981, 178 pp.

[34] Lacis, A., Hansen, **J.,** Lee, P., Mitchell, T. Lebedeff, G. effect of trace gases, 1970–80. ***Geophys. Res. Lett.,*** 1981, **8** (l0), 1035-8.

[35] Mitchell, C. **S.,** Potter, G. L., Ellsaesser, H. W. & Walton, J. J. 'Case study of feedbacks and synergisms in a doubled CO2 experiment'. J. ***Atmosph. Sci.,*** 1981, ***38*** (9), 1906-10.